

Shining Light on Carbon Dots: A Biocompatible Approach to Potent Antibacterial Activity and Biofilm Disruption

Qingsong Zhang¹, Jianxin Fu¹, Hong Lin¹, Guanhua Xuan¹, Weiwei Zhang², Lingxin Chen³, and Guoqing Wang¹

¹Ocean University of China

²Ningbo University

³Yantai Institute of Coastal Zone Research

April 27, 2024

Abstract

In spite of tremendous efforts dedicated to addressing bacterial infections and biofilm formation, the post-antibiotic era continues to witness a gap between the established materials and an easily accessible yet biocompatible antibacterial reagent. Here we show carbon dots (CDs) synthesized via a single hydrothermal process can afford promising antibacterial activity that can be further enhanced by exposure to light. By using citric acid and polyethyleneimine as the precursors, the photoluminescence CDs can be produced within one-pot, one-step hydrothermal reaction in only 2 h. The CDs demonstrate robust antibacterial property against both Gram-positive and Gram-negative bacteria and, notably, a considerable enhancement of antibacterial effect can be observed upon photo-irradiation. Mechanistic insights reveal that the CDs generate singlet oxygen (1O_2) when exposed to light, leading to an augmented reactive oxygen species level. The approach for disruption of biofilms and inhibition of biofilm formation by using the CDs has also been established. Our findings present a potential solution to combat antibacterial resistance, and offer a path to reduce dependence on traditional antibiotics.

Shining Light on Carbon Dots: A Biocompatible Approach to Potent Antibacterial Activity and Biofilm Disruption

Qingsong Zhang,¹Jianxin Fu,¹ Hong Lin,¹ Guanhua Xuan,^{*,1} Weiwei Zhang,² Lingxin Chen³ Guoqing Wang,^{*,1,4}

¹ *State Key Laboratory of Marine Food Processing & Safety Control, College of Food Science and Engineering, Ocean University of China, 1299 Sansha Road, Qingdao 266404, China*

² *College of Marine Sciences, Ningbo University, Ningbo 315211, China*

³ *CAS Key Laboratory of Coastal Environmental Process and Ecological Remediation, Research Center for Coastal Environmental Engineering and Technology, Yantai Institute of Coastal Zone Research, Chinese Academy of Sciences, Yantai 264003, China*

⁴ *Laboratory for Marine Drugs and Bioproducts of Qingdao National Laboratory for Marine Science and Technology, Qingdao 266237, China*

Email: xuanguanhua@ouc.edu.cn; gqwang@ouc.edu.cn

Abstract

In spite of tremendous efforts dedicated to addressing bacterial infections and biofilm formation, the post-antibiotic era continues to witness a gap between the established materials and an easily accessible yet

biocompatible antibacterial reagent. Here we show carbon dots (CDs) synthesized via a single hydrothermal process can afford promising antibacterial activity that can be further enhanced by exposure to light. By using citric acid and polyethyleneimine as the precursors, the photoluminescence CDs can be produced within one-pot, one-step hydrothermal reaction in only 2 h. The CDs demonstrate robust antibacterial property against both Gram-positive and Gram-negative bacteria and, notably, a considerable enhancement of antibacterial effect can be observed upon photo-irradiation. Mechanistic insights reveal that the CDs generate singlet oxygen ($^1\text{O}_2$) when exposed to light, leading to an augmented reactive oxygen species level. The approach for disruption of biofilms and inhibition of biofilm formation by using the CDs has also been established. Our findings present a potential solution to combat antibacterial resistance, and offer a path to reduce dependence on traditional antibiotics.

KEYWORDS

carbon dot, one-step reaction, photoactivation, biofilm, antibacterial mechanism

1 INTRODUCTION

The recent pandemic has once more underscored the substantial potency, swift and extensive dissemination, and the threat to human health posed by microorganisms. In particular, the infections of bacterial pathogen continue to be a problem of public health concern.^[1] Recent estimates further suggest that up to 80% of bacterial and archaeal cells reside in biofilms, in which bacteria display characteristics and behavior distinct from their planktonic counterparts.^[2] It has been reported that bacteria in biofilms are 10–1000 times more tolerant of bactericidal reagents than the planktonic counterparts.^[3] Therefore, addressing the resulting recalcitrant infection of pathogenic bacteria and biofilm formation has been the central to health care, veterinary, and disease prevention and control.^[4, 5] Antibiotics are widely used weapons against bacterial infection, but they have been losing their punch due to the emergence and propagation of drug-resistance, caused by their overuse and abuse.^[1, 6] In 2019, approximately 4.95 million people worldwide deaths were linked to bacterial antibiotic resistance.^[7] Furthermore, by 2050, antibiotic-resistant bacterial infections were estimated to annually cause up to 10 million deaths worldwide, and a loss of over 3.8% of the global gross domestic product.^[8, 9]

Nanostructured materials have gained popularity in the post-antibiotic era, due to their associated unique properties.^[9, 10] It has been recognized that nanomaterials hardly causes antibiotic resistance while exhibiting long-lasting antibacterial activity.^[11] Recently, people have evolved to exploit nanomaterials as an alternative to combat bacterial infection, including antibacterial nanomaterials.^[9] Up to date, noble metal (e.g., Ag^[12] and Au^[13]) nanoparticles and metal oxide (e.g., ZnO,^[14] CuO,^[15] and TiO₂,^[16]) nanoparticles have been employed as antimicrobial reagents, attributable to the associated reactive ion release, photocatalytic activity, reactive oxygen species (ROS) generation, and/or physical contact with bacterial cells.^[17] However, most of these nanomaterials are associated with high production expenses and/or the potential emission of toxic substances that can pose a health threat to human beings and the nature. In addition, researchers from microbial and biomedical fields may encounter with synthetic difficulty of nanomaterials and, therefore, the antibacterial applications of nanomaterials has remained limited.^[18] The welfare of humans, animals, and the ecosystem are still pointing to the pressing need for the development of effective yet biocompatible nanomaterials to combat resistant strains and biofilms across various contexts.

As an emerging class of nanomaterials, carbon dots (CDs) can be converted from various carbon sources of wide availability. Interestingly, they have demonstrated their antibacterial property.^[19] Nevertheless, the currently adopted procedures for synthesis of CDs are time-consuming and complicated, making them less accessible to people without synthesis background.^[20] Further, their antibacterial mechanisms are not as well studied as some other materials, such as Ag and metal oxide nanoparticles. Here we showcase the synthesis of tiny yet uniform CDs with a quasi-spherical shape and a size of 3.3 nm through a one-pot, one-step hydrothermal process. The use of citric acid and polyethyleneimine as the precursor are responsible to the resultant positively charged surface, facilitating the interaction with bacterial cells and implement of antibacterial effect. The insights into the bactericidal activity of the CDs elucidate the damaged

bacterial membrane structure and elevated ROS level inside bacterial cells in the presence of the CDs. In particular, a great enhancement in their antibacterial activity is observed, which can be ascribed to the generation of $^1\text{O}_2$ by the CDs under light irradiation. We further demonstrated the negligible cytotoxicity of the CDs even at high concentration, and their capability of efficient elimination of biofilms, making them superior candidates for antibacterial applications in fields ranging from food packing, woundplast production, antibacterial medical device coating, and home sterilizing spray as well.

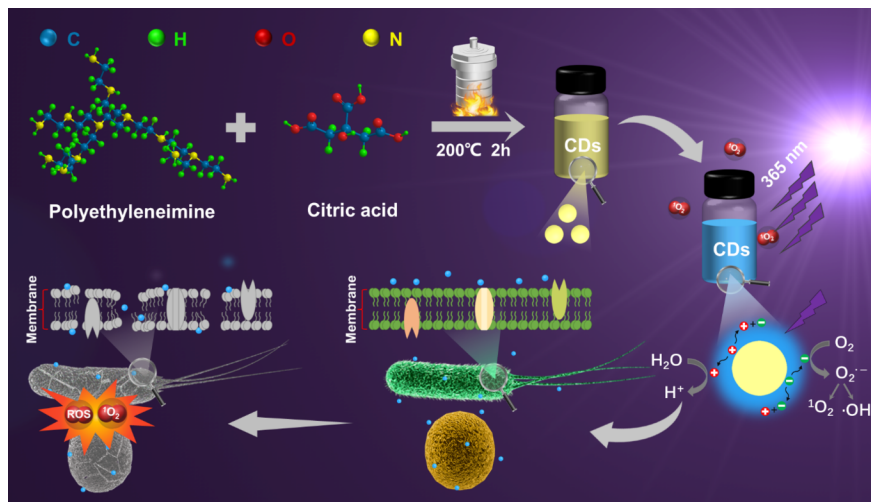


Figure 1. Schematic illustration of the preparation of the CDs with photoactivated antibacterial effect. The positively charged CDs prepared within a hydrothermal reaction cause disruption of the membrane structure of bacteria. Further, $^1\text{O}_2$ is generated by the CDs under light irradiation, which elevate the ROS level and cause enhanced oxidative damage to bacteria.

2 MATERIALS AND METHODS

2.1 Synthesis of the CDs

The CDs were synthesized by a one-step hydrothermal method using CA and PEI (M. W. = 10k) as the raw materials, as shown in **Figure 1**. In brief, CA (1.0 g) and PEI (2.0 g) were dissolved in water (10 mL). Then, the mixture was transferred into a Teflon-lined hydrothermal reactor and reacted at 200°C for 2 h. After cooling to room temperature, the system appearing yellow was dialyzed against water for 24 h with a dialysis bag (1000 Da). Finally, the filtrate was lyophilized to obtain a yellow powder of the CDs.

2.2 Assay of antimicrobial photodynamic inactivation

E. coli and *S. aureus* were used as the model bacteria for the assay of antimicrobial photodynamic inactivation using the spread plate method. A series of the CD solutions at different concentrations were mixed with the *E. coli* or *S. aureus* suspension diluted in PBS (10^6 CFU/mL) at a volume ratio of 1:1 to give a final volume of 2 mL in each well of the 24-well plate. Subsequently, the plate was exposed to a UV lamp (365 nm, 16 W) at a distance of 30 cm from the top of the plate. This condition was applied to all UV irradiation experiments in this work unless specified. After the irradiation, 100 μL of the bacterial suspension ($1\times$) from each well were diluted 5 times in succession with PBS, so that the concentration of the suspension was diluted to $10^{-5}\times$ with an interval of 10^{-1} . Each diluted sample was spread evenly on LB agar plates and incubated at 37°C for 24 h. The photodynamic inactivation of bacteria by the CDs was assessed by the bacterial survival rate, which can be described as follows:

$$\text{Bacterial survival rate (\%)} = (\text{Colony Number}_{(\text{CD})} / \text{Colony Number}_{(\text{control})}) \times 100 \quad (1)$$

where colony number_(CD) represents the number of bacterial colony formed in the presence of the CDs, and colony number_(control) denotes that in the absence of the CDs. In parallel, the survival rate of the bacteria in the dark was also evaluated.

2.3 Cytoplasmic membrane permeability

The permeability of cytoplasmic membrane was assessed by measuring β -galactosidase activity in bacteria using ONPG, a substrate for cytoplasmic β -galactosidase.^[21] Briefly, *E. coli* or *S. aureus* were cultured separately in MHB medium containing 2% lactose until the logarithmic growth phase. Then, the *E. coli* or *S. aureus* suspension was centrifuged and washed with HEPES (5 mM, pH 7.4) containing 20 mM glucose and 2 mM ONPG. Next, 100 μ L of the bacterial suspension (10^6 CFU/mL) was mixed with the CDs (100 μ L) at a predetermined concentration in a 96-well plate. The absorbance of the mixture at 420 nm was subsequently measured at different times with a 5 min interval.

2.4 Quantification of intracellular ROS

Bacterial intracellular ROS level was measured using 2',7'-dichlorofluorescent diacetate (DCFH-DA) as the fluorescent probe.^[22] Briefly, the *E. coli* or *S. aureus* in logarithmic growth phase was centrifuged and washed with PBS. Next, 100 μ L of the bacteria suspended in PBS ($OD_{600\text{ nm}} = 0.2$) was mixed with the CD solution (100 μ L) at a predetermined concentration in a 96-well plate. Subsequently, the 96-well plate was exposed to UV irradiation for 30 min. The suspension was then spiked with DCFH-DA at a final concentration of 10 μ M, followed by incubation for another 30 min in the dark. The fluorescence intensity at 525 nm of the mixture was measured at an excitation wavelength of 496 nm using the microplate reader. The change in ROS level was assessed using the rate of increase (F/F_0) in the fluorescence intensity upon incubation with the CDs, in which F is the fluorescence intensity of the system containing the CDs and F_0 is that without incubating with the CDs. A bacterial suspension to which 1 mM of H_2O_2 was added instead of the CDs was used as a positive control. In parallel, the bacterial intracellular ROS levels upon addition of the CDs in the dark were evaluated.

2.5 Detection of singlet oxygen (1O_2)

Singlet oxygen was determined using 1,3-diphenylbenzofuran (DPBF) as the indicator probe.^[23] Briefly, DPBF and the CDs were dissolved in methanol to give a final concentration of 100 μ M and 100 μ g/mL, respectively, followed by mixing of the both solutions. The mixture (0.5 mL) was either irradiated by UV or left in the dark, and the absorbance at 410 nm was measured, to probe the oxidation of DPBF.

2.6 Biofilm formation and the CDs-induced biofilm disruption

First, 200 μ L of the *S. aureus* or *S. typhimurium* suspension (10^6 CFU/mL) was added to a well from a sterile 96-well plate. Subsequently, the suspension was incubated at 37°C for 48 h, after which the well was rinsed with PBS to obtain *S. aureus* or *S. typhimurium* biofilms. Thus-prepared *S. aureus* or *S. typhimurium* biofilms were separately incubated for 30 min at room temperature with the CD solution at different concentrations under UV irradiation. The mixture was then continued to incubate at 37°C in the dark for 48 h. Each well was rinsed with PBS, stained with crystalline violet (1 wt%). Again, each well was rinsed with PBS, followed by incubation with ethanol (95%). Finally, the absorbance of the solution at 590 nm was measured to quantify the extent of biofilm damage by the CDs. In parallel, the disruption effect of the CDs on biofilm in the dark was also evaluated by room temperature incubation in the dark for 30 min, and then incubation at 37°C in the dark for 48 h.

2.7 Inhibition of biofilm by the CDs

A suspension (100 μ L) of *S. aureus* or *S. typhimurium* of 10^6 CFU/mL in concentration was added to a well from a sterile 96-well plate, to which a CD solution (100 μ L) at a predetermined concentration was added. Subsequently, the mixture was exposed to UV irradiation for 30 min, and then incubated at 37°C for 48 h. Finally, the inhibitory effect of the CD on biofilm was evaluated by crystalline violet staining,

as described above. The inhibitory effect of the CDs on biofilm in the dark was also evaluated under the identical conditions, except for the exemption of UV irradiation.

3 RESULTS AND DISCUSSION

3.1 Synthesis and characterizations of the CDs

The water-soluble CDs were prepared by a simple one-step hydrothermal method using CA and PEI as the raw materials, as shown in **Figure 2a**. CA as an organic acid is widely distributed in nature, and can also be synthesized in large quantities, occupying an important position in the food industry.^[24] PEI is rich in amino groups, which may render the product a positive charge.^[25] After the hydrothermal reaction, a brown solution was obtained. The TEM image of the synthetic product reveals that the small particles are in good mono-dispersity and possess an amorphous structure. Statistical analysis indicates an average diameter of 3.3 nm for the small particles, with a relatively narrow size distribution (**Figure 2b**). As shown in **Figure 2c**, the small particles appear to be light yellow in color under ambient light irradiation at a lower concentration, consistent with the occurrence of the absorption band centered at 351 nm and a shoulder peak at 235 nm. The peak at 235 nm may be attributed to the π - π^* leap of C=C in the particle core.^[26] Under the excitation of UV light, interestingly, a strong blue fluorescence could be seen from the solution, a consequence of the emission of the small particles. With the excitation wavelength increasing from 305 to 425 nm, the emission wavelength shifts from 435 nm to 475 nm, with the maximum intensity occurring under the excitation at 365 nm. The QY under excitation at 365 nm was calculated to be 18.6%. The excitation wavelength-dependent fluorescence emission property of the small particles can be attributed to the presence of different surface states, including functional groups and surface defects.^[27]

The functional group and chemical composition of the particles were further analyzed by FTIR and XPS. As shown in the FTIR spectra (**Figure 2d**), stretching vibrations of O-H/N-H (3450 - 3100 cm^{-1}), $-\text{CH}_3/-\text{CH}_2-$ (3000 - 2700 cm^{-1}), C=O/C=N/C=C (1755 - 1670 , 1690 - 1640 and 1680 - 1620 cm^{-1}), C-N (1420 - 1350 cm^{-1}), and O-C-O (1130 - 1060 cm^{-1}) can be observed. These FTIR peaks are in line with those of the previously reported CDs.^[23] The FTIR characterization also rationalized the occurrence of the absorption peak at 351 nm, which can be ascribed to the n - π^* leap of C=O in the surface defects.^[28] The XPS spectra pointing to a carbon atomic percentage of 68.81% validate the dominant formation of the CDs (**Figure 2e**). The other major elements involve N (19.57%) and O (11.62%). The high-resolution C 1s spectrum that is centered at 283.9 eV displays peaks at 284.7, 286.3 and 287.2 eV, attributable to C=C/C-C, C-N/C-O and C=N bonds,^[29] respectively (**Figure S1**). The high-resolution N1s curve centered at 397.8 eV exhibits peaks at 398.7, 399.8 and 401.1 eV, which can be assigned to C-N-C, N-(C)₃ and N-H bonds,^[30] individually (**Figure S2**). Collectively, the FTIR and XPS results indicate that the synthetic products have various bonds and functional groups. To test the surface charge property of the CDs, the zeta potential of the synthetic products was analyzed. A zeta potential of +13.4 mV (**Figure S3**) may be ascribed to the presence of abundant amino group on the surface.

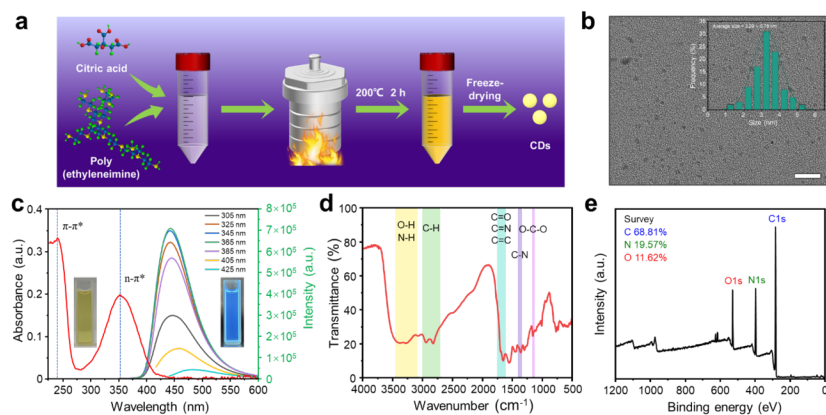


Figure 2. Synthesis and characterizations of the CDs. (a) Cartoon of the synthesis of the CDs by the one-step hydrothermal method. (b) A typical TEM image of the CDs. Inset shows the particle size distribution of the CDs. Scale bar: 25 nm. (c) Absorption spectrum of the CDs, and the photoluminescence spectra under different excitation conditions. Inset shows the digital photographs of the CD solution under ambient irradiation (left) and a 365 nm-UV irradiation (right). (d) FTIR spectrum of the CDs. (e) XPS spectrum of the CDs.

3.2 The antibacterial property and antibacterial mechanisms of the CDs

To evaluate the antibacterial activity of the CDs, *E. coli*, *S. aureus*, *P. aeruginosa*, *S. typhimurium*, and *V. parahaemolyticus* strains were utilized as the model bacteria. The antibacterial property of the CDs for each bacterium was tested in the dark using the spread plate method. As shown in **Figure S4**, the number of colonies decreased drastically with the increase in the concentration of the CD. A broad-spectrum antibacterial capacity of the CDs was therefore demonstrated.

Due to the electrostatic action, the positively charged CDs may complex with the membrane upon adsorption on bacteria, which alters the fluidity of the lipid bilayer and destroy the membrane structure for antibacterial purposes.^[31] ONPG was used to assess the permeability of the cytoplasmic membranes of *E. coli* and *S. aureus*. It is recognized that when the cytoplasmic membrane is disrupted, β -galactosidase is released from the cell and catalyzes the hydrolysis of ONPG to produce the yellow o-nitrophenol.^[32] As shown in **Figure 3a**, the absorbance at 420 nm increased gradually with the increase in the CD concentration and incubation time, although the rate of increase slowed down after around 30 min. This indicates that the permeability of the cytoplasmic membranes of *E. coli* was positively correlated with the concentration of the CDs and incubation time. Similar results were attained for the *S. aureus* group (**Figure 3b**). Noteworthy, higher concentrations of the CD were required for *S. aureus* to cause a consequence of cytoplasmic membrane damage comparable to that of *E. coli*. This result can be ascribed to the thicker cytoderm of *S. aureus* that is composed of peptidoglycan, in comparison with that of *E. coli*.^[33] The above results suggest that the CDs disrupt the bacterial cytoplasmic membrane.

To directly visualize the disrupted bacterial structure by the CDs, the morphological change in *E. coli* and *S. aureus* were studied using electron microscopies. As shown in the SEM images, *E. coli* in the control group possessed a smooth surface with an intact cell wall and a well-stereo-shaped body, while the bacterial cell walls treated with the CDs became rough and displayed obvious wrinkles and damage (**Figure 3c**). The TEM images further confirmed the disruption of *E. coli* structure caused by the CDs (**Figure 3d**). *E. coli* treated with the CDs demonstrated significant morphological change, and the intracellular content appeared to ooze out. Similar phenomena were observed for *S. aureus*. Both the SEM and TEM characterizations reveal that *S. aureus* treated with the CDs had severe surface structural damage and clear leakage of intracellular content. The above result indicates that the disruption of the membrane structure by the CDs may be responsible for the bacteria leakage and the bacteria-killing effect (**Figure 3e**).

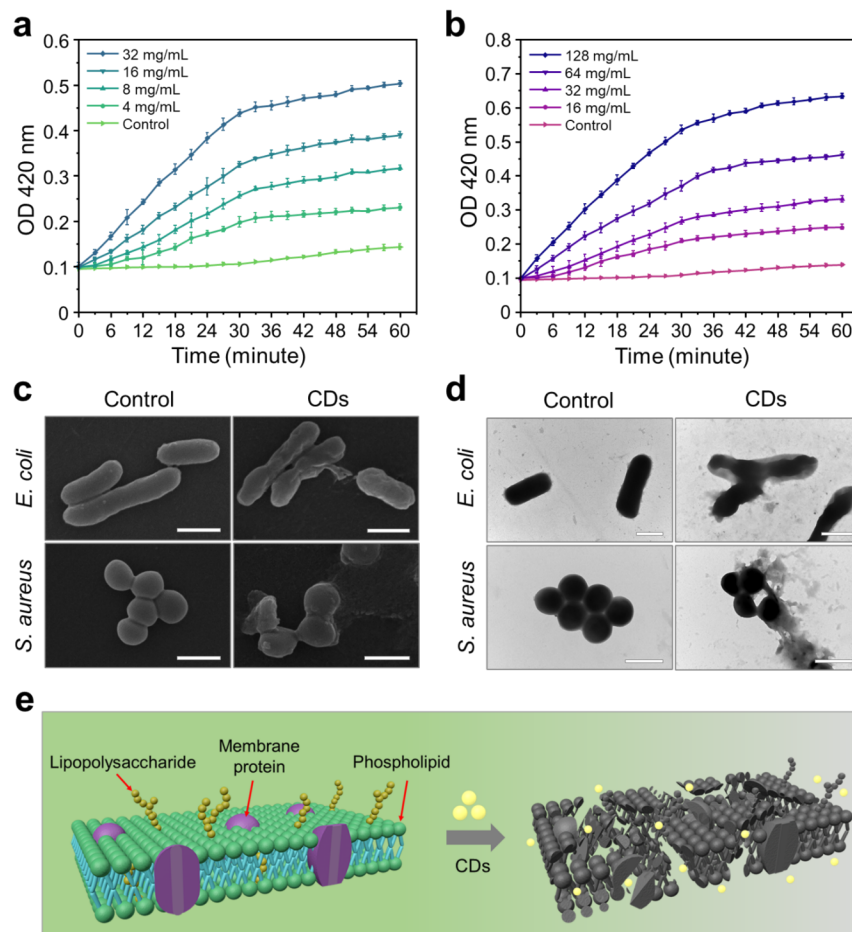


Figure 3. The effects of the CDs on bacterial cell membranes. (a-b) Time courses of the absorbance at 420 nm of the mixtures of the CD at different concentrations with *E. coli* (a) and *S. aureus* (b) in the presence of ONPG. The absorbance at 420 nm on the y-axis is proportional to the amount of leaked β -galactosidase. (c-d) SEM (c) and TEM (d) images of *E. coli* and *S. aureus* before and after the treatment by 50 mg/mL of the CD for 1 h. Scale bars all indicate 1 μ m. (e) Schematic illustration of the disruption of the bacteria membrane structure by the CDs.

3.3 Photodynamic antimicrobial activity of the CDs and effect on ROS levels

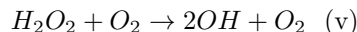
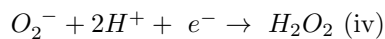
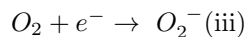
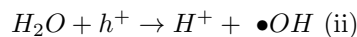
It has been reported that CDs with superior optical property can induce phototoxic reactions under light irradiation, which we think may be capable of photodynamic killing of bacteria.^[34] To this end, we further investigated if the antibacterial effect of the CDs could be enhanced under 365 nm-UV light (Figure 4a). The result shows that compared with that with the non-luminescent CDs (Figure 4b), the UV light irradiation (Figure 4c) made a negligible light effect on the survival rate of *E. coli*; while the bacterial survival rate was greatly reduced under light irradiation. It has been indeed reported that the CDs can initiate the efficient charge separation under photoirradiation.^[35] Therefore, it is deducible that the photoinduced redox potential facilitates the transfer of charge or energy to a substance or to molecular oxygen to produce more ROS, and causes aggravated damage to the bacteria.^[34, 36]

In addition, the survival rate of *E. coli* strongly depends on CD concentration and incubation time. The higher the concentration of the CDs, the lower the survival rate. A similar trend was confirmed with increasing incubation time. The reduced survival rate of *E. coli* with increasing the CD amount and incubation

time can be rationalized by the sufficient production and accumulation of ROS under the conditions. Similar results were attained for the *S. aureus* group under dark (**Figure 4d**) or UV light irradiation (**Figure 4e**). Namely, the survival rate of *S. aureus* is also dependent on the concentration and incubation time of the CDs. Therefore, photoirradiation can effectively boost the antibacterial ability of the CD, regardless of the type of bacteria.

As the luminescence of the CDs under light excitation associate with recombination of photoinduced electrons and holes,^[37] a high quantum yield of the CDs may lead to further enhanced antibacterial effect. We next produced CDs in parallel using PEI of different molecular weights, that is 2 kDa, 10 kDa and 25 kDa, respectively, and their quantum yields were calculated to be 5.7, 18.6, and 21.3% (**Figure S5**), respectively. Interestingly, the CDs with a higher quantum yield exhibited a stronger antibacterial effect under the identical treatment conditions, which has been validated for both *E. coli* (Gram-negative) and *S. aureus* (Gram-positive) (**Figure S5**). This can be ascribed to the fact that, upon absorption of photons, the CDs with a higher quantum yield can produce more electrons and holes. This behavior could promote energy transfer to produce active substances such as ROS, exerting greater killing effects.^[38]

We next became interested in the molecular mechanism of the photodynamic killing by the CDs. To test whether the CDs generate ROS under light irradiation, which is the mostly considered cause of bacterial death,^[39] DCFH-DA was used to serve as the probe to detect intracellular ROS, which can be oxidized into highly fluorescent 2',7'-dichlorofluorescein by ROS.^[40] Our results reveal that compared with the *E. coli* group treated in the dark, the CDs under light irradiation produced more ROS, and the generation of ROS was boosted with increasing doses of the CDs (**Figure 4f**). Similar results were attained for the *S. aureus* group (**Figure 4g**). To test whether ¹O₂ is involved in the produced ROS,^[41] DBPF as the indicator was employed. The probing mechanism for ¹O₂ lies in its decomposition by DBPF into 1,2-dibenzoylbenzene, leading to a decrease in UV absorbance intensity.^[42] As shown in **Figure S6**, the absorption peak of the mixture of the CDs and DPBF at 410 nm decreases significantly as the irradiation time increases; whereas no change in the absorbance of the mixture was attained in the dark. We further found that neither the pure CDs nor DPBF exhibit a decay in absorbance at 410 nm, regardless of whether there was a light (**Figure 4h**). The results point to the generation of ¹O₂ by the CDs under light irradiation. Indeed, the CDs undergo charge separation upon photoexcitation, and generate electrons and holes on the CDs to drive redox reactions listed below, a phenomenon similar to those observed in semiconductor nanomaterials.^[43]



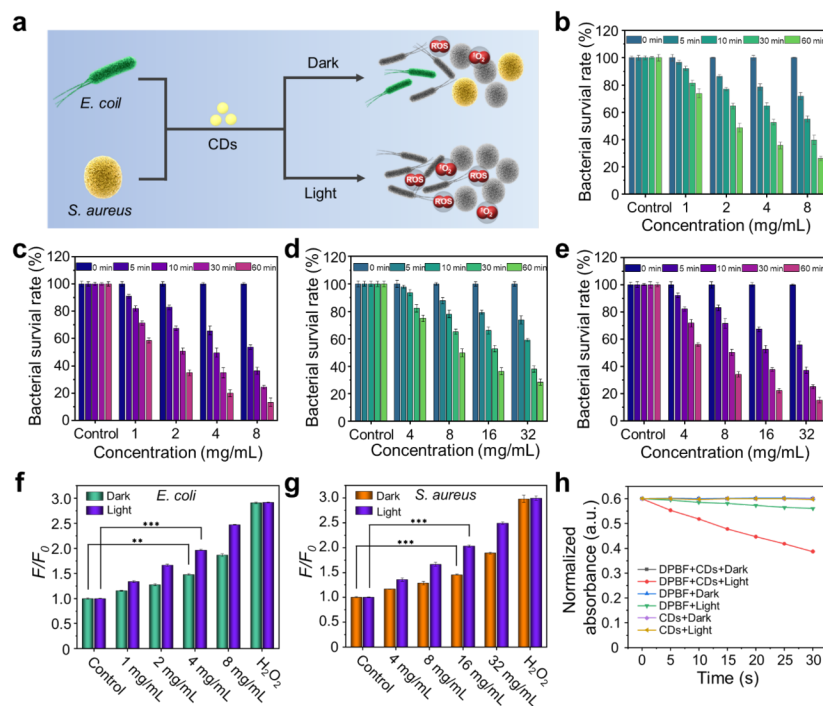


Figure 4. Photodynamic antimicrobial activity of the CDs. (a) Schematic illustration of the antibacterial effect of the CDs on *E. coli* and *S. aureus* under different conditions. (b-c) Comparison of bacterial survival rate of *E. coli* upon treatment with different concentrations of the CD for different times in the dark (b) and under light irradiation (c). (d-e) Comparison of bacterial survival rate of *S. aureus* upon treatment with different concentrations of the CD at different times in the dark (d) and in the light irradiation (e). (f-g) ROS levels of *E. coli* (f) and *S. aureus* (g) upon treatment with different concentrations of the CD at 30 min under light irradiation and in the dark. The groups treated with H₂O₂ were used as the positive control. (h) Time courses of the normalized absorbance at 410 nm of the CDs, DPBF, and the mixture of the CDs and DPBF under light irradiation and in the dark. Note that the CD and DPBF used in the corresponding samples were of 100 μg/mL and 100 μM in final concentration, respectively.

3.4 Effect of the CDs on biofilms

Biofilms can provide physical barriers for bacteria, and enhance antibiotic resistance, making it even more difficult to kill.^[3] We further employed the CDs in a trial of biofilm elimination using *S. aureus* and *S. typhimurium* as the model bacteria, which are both foodborne pathogens that can produce biofilms.^[44] They have been recognized as an important food safety issue causing huge economic losses in the food industry.^[45] The crystal violet-staining method was used to assess the extent of damage to the biofilms by the CDs,^[46] in which crystal violet binds to lipid molecules in the biofilms *via* hydrogen bonding and electrostatic interaction. The occurrence of the purple solution shown in **Figure 5** is attributed to the alcohol-induced disruption of the interactions, and subsequently the shedding of the crystal violet from the biofilms. The absorbance of the solution at 590 nm gradually decreases with increasing amount of the CD in the concentration range of 1-50 mg/mL, consistent with the lighter color of the solution (**Figure 5a**). This indicates that the CDs could destroy the *S. aureus* biofilms in a concentration-dependent manner over a range of concentrations. Though the absorbance of the CD-treated biofilm system decreases no matter under light or in the dark, there is a photo-enhancement effect on the disruption of the biofilm by the CDs. When the concentration of the CD was 10 mg/mL, the extent of damage for the *S. aureus* biofilm was enhanced by 22% with the photo-activated CDs. The absorbance remains almost unchanged when the CD concentration reaches 50

mg/mL, indicative of a saturation effect for the concentration of the CDs. Under the condition, the *S. aureus* biofilm was disrupted in a percentage of as high as 83.2%. Similar results were attained for the *S. typhimurium* group (**Figure 5b**). Notably, when the concentration of the CDs was 10 mg/mL, there was a strong photosensitization of the CDs, boosting the damage of the *S. typhimurium* biofilm by about 17.8% compared with that in the dark.

By treating bacteria with the CDs at early stages, we also discovered that the CDs could inhibit biofilm formation. **Figure 5c** shows the absorbance at 590 nm decreases with increasing the CD concentration in the range of 1-20 mg/mL. Further, there is still a photo-enhancement effect on the inhibition of biofilm formation by the CDs. The CDs could enhance the inhibition to the formation of *S. aureus* biofilm by 34.5% under irradiation at the concentration of 15 mg/mL. The photoactivated inhibition was nearly saturated at the concentration of 20 mg/mL, whereas a much higher one (30 mg/mL) was required to achieve a similar consequence in the dark, agreeing very well with the digital photo results. Interestingly, the CDs could inhibit *S. aureus* biofilm formation in an extent of about 95.9% under irradiation at a concentration of 20 mg/mL. We observed similar results for the *S. typhimurium* group (**Figure 5d**). It is further inferred that the CD at a concentration of 15 mg/mL could inhibit *S. typhimurium* biofilm formation in a rate of approximately 97.5% under irradiation. We therefore suggest that the CDs afford high potential in both effective disruption and inhibition of biofilm (**Figure 5e**). On the other hand, the inhibition of biofilm by the CDs is likely more effective than the disruption. This result can be ascribed to the ease of killing bacteria at the early stage of biofilm formation, in which no compact extracellular polymeric substances around the bacteria are produced yet.^[47] Furthermore, the CDs are featured with low cytotoxicity. A minor decrease in cell viability (~92%) was observed after incubation for 24 h at a CD concentration of 100 mg/mL (**Figure S7**), indicative of a good balance of high antibacterial activity and low toxicity.

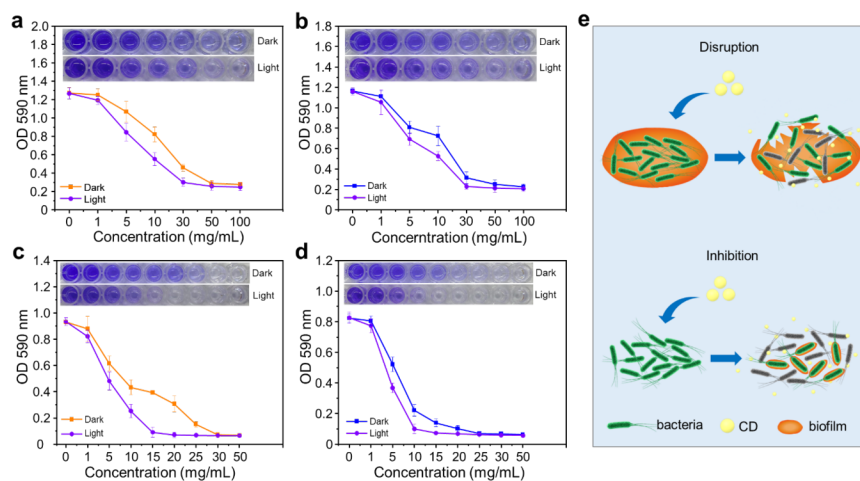


Figure 5. Evaluation of the effect of the CDs on biofilms. (a-b) The absorbance of the crystal violet stained solutions at 590 nm after treatment of *S. aureus* (a) and *S. typhimurium* (b) biofilms with different concentrations of the CD for 48 h under light irradiation and in the dark. Inset shows the corresponding photographs of the crystal violet stained solutions after treatment of *S. aureus* (a) and *S. typhimurium* (b) biofilms with different concentrations of the CD for 48 h under irradiation and in the dark. (c-d) The absorbance of the crystal violet stained solutions at 590 nm after treatment of *S. aureus* (c) and *S. typhimurium* (d) with different concentrations of the CD for 48 h under light and in the dark. Inset denotes the corresponding photographs of crystal violet stained suspensions after treatment of *S. aureus* (c) and *S. typhimurium* (d) with different concentrations of the CD for 48 h under irradiation and in the dark. Note that the concentration of the CD in each well in all the photographs corresponds to that of the *x*-axis towards below. (e) Schematic illustration of the disruptive and inhibitory effects of the CDs on biofilm.

4 CONCLUSIONS

The swift proliferation of antibiotic resistance has necessitated the development of antibacterial materials that afford excellent antibacterial property while enjoying universal recognition akin to antibiotics. In this study, a new type of CDs with photodynamic and synergistic antibacterial effect is synthesized by means of a one-step hydrothermal process, offering a new train of thought for combating antibiotic resistance. Apart from the ROS intrinsically generated by the CDs, evolution of singlet oxygen ($^1\text{O}_2$) can also be triggered by the CDs under light irradiation, contributing to a photoinduced synergistic bactericidal activity. The CDs possess three advantages over the previously reported antibacterial materials. By using citric acid and PEI as the precursor, first, the tiny (~ 3 nm) yet uniform CDs can be produced in 2 h in a single-step, one-pot fashion. The procedure may be achievable without the need for a professional background. Second, the CDs afford enhanced antibacterial effect with broad-spectrum effectiveness under photoirradiation, depending upon their quantum yield that is tunable with the molecular weight of PEI. Mechanistic insights into the antibacterial effect reveal the CDs-induced disruption of bacterial membrane and elevation of intracellular ROS level. Third, the CDs exert minimal cytotoxicity even at a concentration of 100 mg/mL, pointing to a high biocompatibility. This makes the CDs particularly useful for applications in the fields of food packing, antibacterial coating of medical devices and pharmaceuticals. Given the synthetic accessibility and wide availability of carbon sources, we suggest that the CDs be prepared in a scalable and lower-cost way from waste organic materials. We also hope that our findings will inspire more efforts on creation of promising materials as potent antibacterial agents, which can combat bacterial infections and biofilms while overcoming antibiotic resistance.

AUTHOR CONTRIBUTIONS

Qingsong Zhang performed data curation, investigation, and writing – original draft. Jianxin Fu performed data curation. Hong Lin performed project administration. Guanhua Xuan performed conceptualization, investigation, and methodology. Weiwei Zhang performed conceptualization, and supervision. Lingxin Chen performed supervision. Guoqing Wang performed funding acquisition, methodology, and writing – review and editing.

ACKNOWLEDGMENTS

This work was supported by National Natural-Science Foundation of China (No.32373172), and a Special Fund for the Qingdao Science and Technology Program of Public Wellbeing (22-3-7-cspz-4-nsh).

CONFLICT OF INTEREST STATEMENT

The authors declare no competing financial interest.

DATA AVAILABILITY STATEMENT

The data that support the findings of this study are available from the cor-responding author upon reasonable request.

SUPPORTING INFORMATION

Additional supporting information can be found online in the Support-ing Information section at the end of this article.

REFERENCES

1. Organization, W.H. (2022). Global antimicrobial resistance and use surveillance system (GLASS) report 2022. *WHO: Geneva* .
2. Penesyan, A., Paulsen, I.T., Kjelleberg, S., & Gillings, M.R. (2021). Three faces of biofilms: A microbial lifestyle, a nascent multicellular organism, and an incubator for diversity. *npj Biofilms and Microbiomes* , 7 , 80.

3. Vishwakarma, A., Dang, F., Ferrell, A., Barton, H.A., & Joy, A. (2021). Peptidomimetic polyurethanes inhibit bacterial biofilm formation and disrupt surface established biofilms. *Journal of the American Chemical Society* , *143* , 9440-9449.
4. Koo, H., Allan, R.N., Howlin, R.P., Stoodley, P., & Hall-Stoodley, L. (2017). Targeting microbial biofilms: current and prospective therapeutic strategies. *Nature Reviews Microbiology* , *15* , 740-755.
5. Chambers, J.R., & Sauer, K. (2013). Small RNAs and their role in biofilm formation. *Trends in Microbiology* , *21* , 39-49.
6. Willyard, C. (2017). The drug-resistant bacteria that pose the greatest health threats. *Nature* , *543* , 15-15.
7. Murray, C.J.L., Ikuta, K.S., Sharara, F., Swetschinski, L., Robles Aguilar, G., Gray, A., Han, C., Bisignano, C., Rao, P., & Wool, E. (2022). Global burden of bacterial antimicrobial resistance in 2019: A systematic analysis. *The Lancet* , *399* , 629-655.
8. Zhang, S., Yang, H., Wang, M., Mantovani, D., Yang, K., Witte, F., Tan, L., Yue, B., & Qu, X. (2023). Immunomodulatory biomaterials against bacterial infections: Progress, challenges, and future perspectives. *The Innovation* , *4* , 100503.
9. Gupta, A., Mumtaz, S., Li, C.H., Hussain, I., & Rotello, V.M. (2019). Combatting antibiotic-resistant bacteria using nanomaterials. *Chemical Society Reviews* , *48* , 415-427.
10. Zhang, L., Ma, X., Wang, G., Liang, X., Mitomo, H., Pike, A., Houlton, A., & Ijro, K. (2021). Non-origami DNA for functional nanostructures: From structural control to advanced applications. *Nano Today* , *39* , 101154.
11. Fan, X., Yang, F., Nie, C., Ma, L., Cheng, C., & Haag, R. (2021). Biocatalytic nanomaterials: A new pathway for bacterial disinfection. *Advanced Materials* , *33* , 2100637.
12. Xie, X., Sun, T., Xue, J., Miao, Z., Yan, X., Fang, W., Li, Q., Tang, R., Lu, Y., Tang, L., Zha, Z., & He, T. (2020). Targeted antibacterial therapy: Ag nanoparticles cluster with pH-triggered reassembly in targeting antimicrobial applications. *Advanced Functional Materials* , *30* , 2070106.
13. Yan, L., Mu, J., Ma, P., Li, Q., Yin, P., Liu, X., Cai, Y., Yu, H., Liu, J., Wang, G., & Liu, A. (2021). Gold nanoplates with superb photothermal efficiency and peroxidase-like activity for rapid and synergistic antibacterial therapy. *Chemical Communications* , *57* , 1133-1136.
14. Izzi, M., Sportelli, M.C., Torsi, L., Picca, R.A., & Cioffi, N. (2023). Synthesis and antimicrobial applications of ZnO nanostructures: A review. *ACS Applied Nano Materials* , *6* , 10881-10902.
15. Gonçalves, R.A., Ku, J.W.K., Zhang, H., Salim, T., Oo, G., Zinn, A.A., Boothroyd, C., Tang, R.M.Y., Gan, C.L., Gan, Y.H., & Lam, Y.M. (2022). Copper-nanoparticle-coated fabrics for rapid and sustained antibacterial activity applications. *ACS Applied Nano Materials* , *5* , 12876-12886.
16. Alotaibi, A.M., Promdet, P., Hwang, G.B., Li, J., Nair, S.P., Sathasivam, S., Kafizas, A., Carmalt, C.J., & Parkin, I.P. (2021). Zn and N codoped TiO₂ thin films: Photocatalytic and bactericidal activity. *ACS Applied Materials & Interfaces* , *13* , 10480-10489.
17. Zhong, Y., Zheng, X., Zhao, S., Su, X., & Loh, X. (2022). Stimuli-activable metal-bearing nanomaterials and precise on-demand antibacterial strategies. *ACS Nano* , *16* , 19840-19872.
18. Vimbela, G.V., Ngo, S.M., Frazee, C., Yang, L., & Stout, D.A. (2017). Antibacterial properties and toxicity from metallic nanomaterials. *International Journal of Nanomedicine* , *12* , 3941-3965.
19. Du, X., Zhang, M., Ma, Y., Wang, X., Liu, Y., Huang, H., & Kang, Z. (2023). Size-dependent antibacterial of carbon dots by selective absorption and differential oxidative stress of bacteria. *Journal of Colloid and Interface Science* , *634* , 44-53.

20. Chen, W., Shen, J., Wang, Z., Liu, X., Xu, Y., Zhao, H., & Astruc, D. (2021). Turning waste into wealth: Facile and green synthesis of carbon nanodots from pollutants and applications to bioimaging. *Chemical Science* , *12* , 11722-11729.
21. Wang, J., Chou, S., Yang, Z., Yang, Y., Wang, Z., Song, J., Dou, X., & Shan, A. (2018). Combating drug-resistant fungi with novel imperfectly amphipathic palindromic peptides. *Journal of Medicinal Chemistry* , *61* , 3889-3907.
22. Chen, M., Zhang, J., Qi, J., Dong, R., Liu, H., Wu, D., Shao, H., & Jiang, X. (2022). Boronic acid-decorated multivariate photosensitive metal-organic frameworks for combating multi-drug-resistant bacteria. *ACS Nano* , *16* , 7732-7744.
23. Nie, X., Jiang, C., Wu, S., Chen, W., Lv, P., Wang, Q., Liu, J., Narh, C., Cao, X., Ghiladi, R.A., & Wei, Q. (2020). Carbon quantum dots: A bright future as photosensitizers for in vitro antibacterial photodynamic inactivation. *Journal of Photochemistry and Photobiology B: Biology* , *206* , 111864.
24. Amato, A., Becci, A., & Beolchini, F. (2020). Citric acid bioproduction: The technological innovation change. *Critical Reviews in Biotechnology* , *40* , 199-212.
25. Godbey, W.T., Wu, K.K., & Mikos, A.G. (1999). Poly (ethylenimine) and its role in gene delivery. *Journal of Controlled Release* , *60* , 149-160.
26. Yang, J., Gao, G., Zhang, X., Ma, Y., Chen, X., & Wu, F. (2019). One-step synthesis of carbon dots with bacterial contact-enhanced fluorescence emission: Fast Gram-type identification and selective Gram-positive bacterial inactivation. *Carbon* , *146* , 827-839.
27. Lee, H., Chiang, P., Wu, H., Wang, T., Yang, T., Cheng, W., Lo, L., & Liao, W. (2022). Versatile azido-functionalized carbon dots for cancer cell imaging. *ACS Applied Nano Materials* , *5* , 12374-12379.
28. Wang, T., Chen, C., Wang, C., Tan, Y., & Liao, W. (2017). Multicolor functional carbon dots via one-step refluxing synthesis. *ACS Sensors* , *2* , 354-363.
29. Liu, M., Chen, B., Li, C., & Huang, C. (2019). Carbon dots: Synthesis, formation mechanism, fluorescence origin and sensing applications. *Green Chemistry* , *21* , 449-471.
30. Liu, S., Tian, J., Wang, L., Zhang, Y., Qin, X., Luo, Y., Asiri, A.M., Al-Youbi, A.O., & Sun, X. (2012). Hydrothermal treatment of grass: A low-cost, green route to nitrogen-doped, carbon-rich, photoluminescent polymer nanodots as an effective fluorescent sensing platform for label-free detection of Cu (II) ions. *Advanced Materials* , *24* , 2037-2041.
31. Pfeiffer, T., De Nicola, A., Montis, C., Carlà, F., van der Vegt, N.F.A., Berti, D., & Milano, G. (2019). Nanoparticles at biomimetic interfaces: Combined experimental and simulation study on charged gold nanoparticles/lipid bilayer interfaces. *The Journal of Physical Chemistry Letters* , *10* , 129-137.
32. Jian, H.J., Wu, R.S., Lin, T.Y., Li, Y.J., Lin, H.J., Harroun, S.G., Lai, J.Y., & Huang, C.C. (2017). Super-cationic carbon quantum dots synthesized from spermidine as an eye drop formulation for topical treatment of bacterial keratitis. *ACS Nano* , *11* , 6703-6716.
33. Zheng, W., Jia, Y., Zhao, Y., Zhang, J., Xie, Y., Wang, L., Zhao, X., Liu, X., Tang, R., Chen, W., & Jiang, X. (2021). Reversing bacterial resistance to gold nanoparticles by size modulation. *Nano Letters* , *21* , 1992-2000.
34. Tiwari, D.K., Jha, G., Tiwari, M., Kerkar, S., Das, S., & Gobre, V.V. (2021). Synergistic antibacterial potential and cell surface topology study of carbon nanodots and tetracycline against *E. coli* . *Frontiers in Bioengineering and Biotechnology* , *9* , 626276.
35. LeCroy, G.E., Yang, S., Yang, F., Liu, Y., Fernando, K.A.S., Bunker, C.E., Hu, Y., Luo, P.G., & Sun, Y. (2016). Functionalized carbon nanoparticles: Syntheses and applications in optical bioimaging and energy conversion. *Coordination Chemistry Reviews* , *320-321* , 66-81.

36. Dong, X., Ge, L., Abu Rabe, D.I., Mohammed, O.O., Wang, P., Tang, Y., Kathariou, S., Yang, L., & Sun, Y. (2020). Photoexcited state properties and antibacterial activities of carbon dots relevant to mechanistic features and implications. *Carbon* , 170 , 137-145.
37. Fernando, K.A.S., Sahu, S., Liu, Y., Lewis, W.K., Gulianti, E.A., Jafariyan, A., Wang, P., Bunker, C.E., & Sun, Y. (2015). Carbon quantum dots and applications in photocatalytic energy conversion. *ACS Applied Materials & Interfaces* , 7 , 8363-8376.
38. Al Awak, M.M., Wang, P., Wang, S., Tang, Y., Sun, Y., & Yang, L. (2017). Correlation of carbon dots' light-activated antimicrobial activities and fluorescence quantum yield. *RSC Advances* , 7 , 30177-30184.
39. Wang, X., Wang, H., Cheng, J., Li, H., Wu, X., Zhang, D., Shi, X., Zhang, J., Han, N., & Chen, Y. (2023). Initiative ROS generation of Cu-doped ZIF-8 for excellent antibacterial performance. *Chemical Engineering Journal* , 466 , 143201.
40. Lyublinskaya, O.G., Ivanova, J.S., Pugovkina, N.A., Kozhukharova, I.V., Kovaleva, Z.V., Shatrova, A.N., Aksenov, N.D., Zenin, V.V., Kaulin, Y.A., Gamaley, I.A., & Nikolsky, N.N. (2017). Redox environment in stem and differentiated cells: A quantitative approach. *Redox Biology* , 12 , 758-769.
41. Maisch, T., Baier, J., Franz, B., Maier, M., Landthaler, M., Szeimies, R.M., & Bäumlner, W. (2007). The role of singlet oxygen and oxygen concentration in photodynamic inactivation of bacteria. *Proceedings of the National Academy of Sciences of the United States of America* , 104 , 7223-7228.
42. Carloni, P., Damiani, E., Greci, L., Stipa, P., Tanfani, F., Tartaglino, E., & Wozniak, M. (1993). On the use of 1,3-diphenylisobenzofuran (DPBF). Reactions with carbon and oxygen centered radicals in model and natural systems. *Research on Chemical Intermediates* , 19 , 395-405.
43. Yu, X., Wang, S., Zhang, X., Qi, A., Qiao, X., Liu, Z., Wu, M., Li, L., & Wang, Z.L. (2018). Heterostructured nanorod array with piezophototronic and plasmonic effect for photodynamic bacteria killing and wound healing. *Nano Energy* , 46 , 29-38.
44. Gkana, E.N., Giaouris, E.D., Doulgeraki, A.I., Kathariou, S., & Nychas, G.-J.E. (2017). Biofilm formation by *Salmonella typhimurium* and *Staphylococcus aureus* on stainless steel under either mono- or dual-species multi-strain conditions and resistance of sessile communities to sublethal chemical disinfection. *Food Control* , 73 , 838-846.
45. Wang, X., Huang, Y., Wu, S., Duan, N., Xu, B., & Wang, Z. (2016). Simultaneous detection of *Staphylococcus aureus* and *Salmonella typhimurium* using multicolor time-resolved fluorescence nanoparticles as labels. *International Journal of Food Microbiology* , 237 , 172-179.
46. Kamimura, R., Kanematsu, H., Ogawa, A., Kogo, T., Miura, H., Kawai, R., Hirai, N., Kato, T., Yoshitake, M., & Barry, D.M. (2022). Quantitative analyses of biofilm by using crystal violet staining and optical reflection. *Materials* , 15 , 6727.
47. Ran, H., Cheng, X., Bao, Y., Hua, X., Gao, G., Zhang, X., Jiang, Y., Zhu, Y., & Wu, F. (2019). Multifunctional quaternized carbon dots with enhanced biofilm penetration and eradication efficiencies. *Journal of Materials Chemistry B* , 7 , 5104-5114.